[CANCER RESEARCH 63, 7400–7409, November 1, 2003]

Vascular Damage and Anti-angiogenic Effects of Tumor Vessel-Targeted Liposomal Chemotherapy[1]

Fabio Pastorino, Chiara Brignole, Danilo Marimpietri, Michele Cilli, Claudio Gambini, Domenico Ribatti, Renato Longhi, Theresa M. Allen, Angelo Corti, and Mirco Ponzoni[2]

Differentiation Therapy Unit, Laboratory of Oncology [F. P., C. B., D. M., M. P.] and Laboratory of Pathology [C. G.], G. Gaslini Children's Hospital, 16148 Genoa, Italy; Animal Research Facility, Istituto Nazionale per la Ricerca sul Cancro, 16100, Genoa, Italy [M. C.]; Department of Human Anatomy and Histology, University of Bari, 70100 Bari, Italy [D. R.]; Istituto di Chimica del Riconoscimento Molecolare, Consiglio Nazionale delle Ricerche, 20131 Milan, Italy [R. L.]; Department of Pharmacology, University of Alberta, T6G 2H7 Edmonton, Canada [T. M. A.]; and Immunobiotechnology Unit, San Raffaele Institute, 20132 Milan, Italy [A. C.]

ABSTRACT

The poor selective toxicity of chemotherapeutic anticancer drugs leads to dose-limiting side effects that compromise clinical outcome. Solid tumors recruit new blood vessels to support tumor growth, and unique epitopes expressed on tumor endothelial cells can function as targets for the anti-angiogenic therapy of cancer. An NGR peptide that targets aminopeptidase N, a marker of angiogenic endothelial cells, was coupled to the surface of liposomal doxorubicin (NGR-SL[DXR]) and was used to treat orthotopic neuroblastoma (NB) xenografts in SCID mice. Pharmacokinetic studies indicated that liposomes coupled to NGR peptide had long-circulating profiles in blood. Their uptake into NB tumor was time dependent, being at least 10 times higher than that of nontargeted liposomes (SL[DXR]) after 24 h, with DXR spreading outside the blood vessels and into the tumors. No uptake was observed into tumors of mice treated with the mismatched peptide ARA-targeted SL[DXR]. Tumor-specific DXR uptake was completely blocked when mice were coinjected with a 50-fold molar excess of the soluble NGR peptide. Adrenal tumor-bearing mice treated with 2 mg/kg/week/×3 of NGR-SL[DXR] partly outlived the control mice ($P < 0.001$), whereas doses > 3 mg/kg/week/×3 were toxic. Histopathological analysis of cryosections taken from treated mice revealed pronounced destruction of the tumor vasculature with a marked decreased in vessel density. Double staining of tumors with terminal deoxynucleotidyl transferase-mediated nick end labeling and antifactor VIII antibody or antihuman NB demonstrated endothelial cell apoptosis in the vasculature, as well as increased tumor cell apoptosis. Moreover, mice injected with 3 mg/kg/week/×3 of NGR-SL[DXR] displayed rapid tumor regression, as well as inhibition of metastases growth ($P = 0.0002$). One day after the third treatment, four of six mice showed no evidence of tumors, and the two others showed a >80% reduction in tumor mass and a >90% suppression of blood vessel density ($P < 0.01$). In contrast, mice treated with ARA-SL[DXR] formed large well-vascularized tumors. Finally, a metronomic administration of NGR-SL[DXR] (1 mg/kg/every other 2 days × 9) induced complete tumor eradication in all animals ($P < 0.0001$). Our strategy markedly enhanced the therapeutic index of DXR and enabled metronomic administration of therapeutic doses. A dual mechanism of action is proposed: indirect tumor cell kill via the destruction of tumor endothelium by NGR-targeted liposomes and direct tumor cell kill via localization of liposomal DXR to the tumor interstitial space. This combined strategy has the potential to overcome some major limitations of conventional chemotherapy.

INTRODUCTION

The targeting of therapeutics to blood vessels, using probes that bind to specific molecular addresses in the vasculature, is a major research area (1–3). The inhibition of tumor growth by attacking the vascular supply of the tumor offers a primary target for therapeutic intervention. Indeed, host endothelial cells are believed to play a central role in tumor growth, progression, and metastasis, acting as the primary building blocks of the tumor microvasculature (4). Because of the angiogenesis dependence of solid tumors, predicted by Folkman (4) ~30 years ago, selective inhibition or destruction of the tumor vasculature (using antiangiogenic or antivascular treatments, respectively) could trigger tumor growth inhibition, regression, and/or a state of dormancy and thereby offer a novel approach to cancer treatment. To date, preclinical studies have convincingly validated the guiding principles of this concept (4, 5).

Vascular targeting offers therapeutic promise for the delivery of drugs (6, 7), radionuclides (8), and genes (9, 10). This approach has the advantage that the delivery vehicle, once in the blood stream, should have direct access to the target endothelial cells. One of the newest and most promising strategies in molecularly guided cancer pharmacology is the development of techniques that can modify the kinetic features of these drugs by encapsulating them at considerable concentrations in high molecular order lipidic vesicles known as liposomes (11). Targeted liposomes [lipid vesicles bearing covalently conjugated antibodies (immunoliposomes) or other targeting moieties like specific peptides] have several advantages over simple antibody-drug conjugates for specific drug delivery (11). Use of internalizing ligands for targeting liposomes allows the encapsulated contents to be delivered to the cytosol through the endosome/lysosome pathway (11, 12).

Endothelial cells in the angiogenic vessels within solid tumors express several proteins that are absent or barely detectable in established blood vessels, including α_v integrins, receptors for angiogenic growth factors, and other types of membrane-spanning molecules such as aminopeptidase N (CD13; Refs. 3, 9, 13). Moreover, we recently showed that different CD13 isoforms are expressed within tumor vessels, normal epithelia, and myeloid cells (14). *In vivo* panning of phage libraries in tumor-bearing mice have proven useful for selecting peptides that interact with proteins expressed within tumor-associated vessels and home to neoplastic tissues (3, 6, 13). Among the various tumor-targeting ligands identified thus far, the NGR peptide, which is the ligand for aminopeptidase N, has proven useful for delivering various antitumor compounds to tumor vessels (6, 7, 15, 16). Thus, it may be possible to develop targeted chemotherapy strategies that are based on selective expression of receptors to these peptides in tumor vasculature.

Virtually, every conventional cytotoxic anticancer drug has been accidentally discovered to have anti-angiogenic effects in various *in vitro* and *in vivo* models (17, 18). Interest in exploiting chemotherapeutics as anti-angiogenics has been stimulated by studies showing that frequent administration of low doses of various chemotherapeutic agents (19, 20) called metronomic dosing (21) or anti-angiogenic chemotherapy (19) can target the tumor vasculature with limited host toxicity. This appears to have interesting precedents in the clinic (22).

Received 8/6/03; accepted 8/20/03.

The costs of publication of this article were defrayed in part by the payment of page charges. This article must therefore be hereby marked *advertisement* in accordance with 18 U.S.C. Section 1734 solely to indicate this fact.

[1] Work supported by the Fondazione Italiana per la lotta al Neuroblastoma and the Associazione Italiana Ricerca Cancro. F. P. is a recipient of a Fondazione Italiana per la lotta al Neuroblastoma fellowship.

[2] To whom requests for reprints should be addressed, at Differentiation Therapy Unit, Laboratory of Oncology, G. Gaslini Children's Hospital, Largo G. Gaslini 5, 16148, Genoa, Italy. Phone: +39-010-5636342; Fax: +39-010-3779820; E-mail: mircoponzoni@ospedale-gaslini.ge.it.

Treatment of NB,[3] the second most common solid tumor in childhood, is successful in less than half of patients with high-risk disease (23). A high vascular index in NB correlates with poor prognosis (24), suggesting dependence of aggressive tumor growth on active angiogenesis. The matrix-degrading enzymes MMP-2 and MMP-9 are elevated in high-risk NB compared with low-risk disease (25, 26) and are expressed in NB cell lines, which themselves induce proliferation of endothelial cells (27), supporting the angiogenic phenotype of this tumor (24, 26). Thus, utilization of anti-angiogenic approaches, by themselves or in combination with passive targeting, could potentially improve the outcome in children with NB and may warrant further study.

Here, we describe a novel combination strategy for achieving a NB antitumor response with a NGR peptide-targeted formulation of liposomal DXR. NGR peptide-targeted liposomal DXR, we hypothesize, binds to and kills angiogenic blood vessels and, indirectly, the tumor cells that these vessels support. The NGR-targeted liposomes can also, we hypothesize, penetrate into the tumor interstitial space and function as a sustained release system, resulting in direct cell kill, including cytotoxicity against cells that are at the tumor periphery and are independent of the tumor vasculature. Our therapeutic formulation caused antitumor activity against already established primary tumors, as well as early-phase metastases by causing the selective apoptosis of tumor endothelial cells and destruction of the tumor vasculature.

MATERIALS AND METHODS

Liposomes Preparation. Nontargeted SLs and peptide-targeted liposomes (NGR-SL and ARA-SL) were synthesized from HSPC:CHOL:DSPE-PEG_{2000}, 2:1:0.1 molar ratio, and HSPC:CHOL:DSPE-PEG_{2000}:DSPE-PEG_{2000}-MAL, 2:1:0.08:0.02 molar ratio, respectively (28). In some preparations, [^{3}H]CHE was added as a nonexchangeable, nonmetabolizable lipid tracer. After evaporation under nitrogen, dried lipid films were hydrated in 25 mM HEPES and 140 mM NaCl buffer (pH 7.4). The hydrated liposomes were sequentially extruded (LiposoFast-basic extruder; Avestin, Inc., Leiden, the Netherlands) through a series of polycarbonate filters of pore size ranging from 0.2 μm down to 0.08 μm to produce primarily unilamellar vesicles. Liposomal size was characterized by dynamic light scattering using a Brookhaven BI90 submicron particle size analyzer (Brookhaven Instruments Corp., Holtsville, NY).

DXR was loaded into liposomes via an ammonium sulfate gradient, as previously reported (28). The loading efficiency of DXR was >95% and liposomes routinely contained DXR at a concentration of 150–180 μg DXR/μmol PL.

To enhance the accessibility of NGR peptide when bound to liposomes and also to permit coupling via a thiol to a maleimido moiety on the liposomes, additional residues were added to the peptide NH_2 terminus to provide the peptide G**NGR**GGVRSSSRTPSDKYC with a NH_2-terminal Cys (29). The peptide G**ARA**GGVRSSSRTPSDKYC was used as control. Peptide was conjugated to the liposomes by mixing freshly prepared liposomes with an equimolar (with respect to maleimide) quantity of peptide at 4°C for 16 h under argon followed by a 10-fold excess of 2-mercapethanol for 1 h to derivatize remaining maleimido groups. Uncoupled peptides were separated from the liposomes by passing the coupling mixture through a Sepharose CL-4B column in HEPES buffer (pH 7.4). The efficiency of coupling was determined by estimating the amount of liposome-associated peptides using the CBQCA Protein Quantification kit (Molecular Probes Europe, Leiden, the Netherlands).

Cell Lines and Cellular Association Studies. To broadly cover the phenotypes exhibited by NB cells *in vitro*, we used five human NB cell lines GI-ME-N, GI-LI-N, HTLA-230, IMR-32, and SH-SY5Y (30). The cell lines KS1767 (human Kaposi sarcoma) and THP-1 (human acute monocytic leukemia) were used in some experiments as controls. All cell lines were grown in RPMI 1640 supplemented with 10% fetal bovine serum, as described previously (30).

The cellular association of liposomes targeted via NGR peptides was analyzed by flow cytometry (FACS), using a FACScan instrument for FACS (Becton-Dickinson Immunocytometry Systems). Aliquots of cells (1×10^6/tube) were incubated for 1 h at 4°C with different formulations of liposome-entrapped DXR (SL, NGR-SL, or ARA-SL). The cells were subsequently washed with PBS and enumerated by FACS. Expression of CD13-binding sites by cultured SH-SY-5Y, THP-1, and KS1767 cells was also measured by FACS, using 1 μg/ml WM15 antibody (PharMingen, San Diego, CA), as reported previously (14).

Orthotopic NB Animal Model. Five-week-old female SCID mice were purchased from Harlan Laboratories (Harlan Italy-S.Pietro al Natisone, Udine, Italy). Mice (six to eight mice/group) were anesthetized and injected with the different NB cell lines (2.5×10^6 cells in 20 μl of HEPES buffer), after laparatomy, in the capsule of the left adrenal gland. The lethality of the method was 0%. Mice were monitored at least two times weekly for evidence of tumor development, quantification of tumor size, and evidence of tumor-associated morbidity. All experiments involving animals have been reviewed and approved by the licensing and ethical committee of the National Cancer Research Institute and by Italian Ministry of Health.

BD and PK Experiments. SCID mice carrying orthotopically implanted NB tumors (mean volume ~100 mm^3) were injected via the tail vein with a single dose of liposomes (0.5 μmol PL/mouse), with or without coupled NGR peptides, containing $\sim 3 \times 10^5$ cpm of the lipid tracer [^{3}H]CHE. At selected time points (2, 12, and 24 h) after injection, mice (three mice/group) were anesthetized and sacrificed by cervical dislocation. A blood sample (100 μl) was collected by heart puncture and counted for the [^{3}H] label in a Packard β-counter. Blood correction factors were applied to all samples (28). BD was determined as described previously (31). Data were expressed as the percentage of injected dose/g of tissue.

Histological Analysis. Paraffin-embedded tissue sections (5 μm) were examined after staining with Mayer's H&E (Sigma Chemical Co., St. Louis, MO). Monoclonal antibodies against the endothelial cell marker, factor VIII (M616; Dako, Glostrup, Denmark) and antihuman NB (NB84a; Dako), were used. Briefly, sections were collected on 3-amino-propyl-triethoxysilane-coated slides, deparaffinized by the xylene-ethanol sequence, rehydrated in a graded ethanol scale and in Tris-buffered saline (pH 7.6), and incubated overnight at 4°C with M616 (1:25 in Tris-buffered saline) or NB84a (1:40) after prior antigen retrieval by enzymatic digestion with Ficin (Sigma Chemical Co.). The immunoreaction was performed with the streptavidin-peroxidase complex (LSAB2; Dako) and Fast Red as a chromogen. TUNEL staining was performed using a commercially available apoptosis detection kit (*In situ* Cell Death Detection, POD; Roche Molecular Biochemicals, Mannheim, Germany) according to manufacturer's instructions.

Determination of Microvessel Area. Two investigators with a computerized image analysis system (Leica Quantimet 5000, Wetzlar, Germany) simultaneously assessed microvessel area. Four to six 250 × magnification fields, covering almost the whole of each three sections (every third section within nine serial sections)/sample, were examined with a 484-intersection point square reticulum ($12.5 \times 10^2/mm^2$) inserted in the eyepiece. Care was taken to select microvessels, *i.e.*, capillaries and small venules from all of the factor VIII-stained vessels. They were identified as transversally sectioned tubes with a single layer of endothelial cells, without or with a lumen (diameter ranging from 3 to 10 μm). Microvessels were counted by a planimetric point-count method with slight modifications, according to which only microvessels transversally cut occupying the reticulum points were counted. Because the microvessel diameter was smaller than the distance between adjacent points, only one transversally sectioned microvessels could occupy a given point. Microvessels transversally sectioned outside the points and those longitudinally or tangentially sectioned were omitted. It was thus sufficiently certain that a given microvessel was counted only once, even in the presence of several of its section planes. As almost the entire section of each of three nonadjacent sections was analyzed/sample and as transversally sectioned microvessels hit the intersection points randomly, the method allowed objective counts.

***In Vivo* Therapeutic Studies.** A total of 2.5×10^6 SH-SY-5Y cells were injected orthotopically in the left adrenal gland of mice. Tumors were allowed to grow for 21 days and then i.v. DXR treatment (free or encapsulated in

[3] The abbreviations used are: NB, neuroblastoma; DXR, doxorubicin; SL, stealth liposome; PL, phospholipid; [^{3}H]CHE, cholesteryl-[1,2-^{3}H-(N)]-hexadecyl ether; FACS, fluorescence-activated cell sorting; TUNEL, terminal deoxynucleotidyl transferase-mediated nick end labeling; IHC, immunohistochemistry; NGR-SL[DXR], NGR-targeted liposomal DXR; PK, pharmacokinetic; BD, biodistribution.

targeted or nontargeted liposomes) was initiated with different doses of DXR/kg every week for 3 weeks (see "Legends" and "Results"). At different time points, mice were sacrificed, and tumors were measured with calipers. Tumor volumes were calculated by the formula $\pi/6\ [w_1 \times (w_2)^2]$, where w_1 represented the largest tumor diameter and w_2 represented the smallest tumor diameter. The body weight and general physical status of the animals were recorded daily, and the mice were terminated when tumor reached 1000–1200 mm^3. Histological evaluation of microscopic metastases was performed for all tissues. Organs were fixed in neutral buffered 10% formalin, processed by standard methods, embedded in paraffin, sectioned at 5 μm, and stained with H&E and for IHC. Weight because of tumor burden was calculated by subtracting the normal wet organ weight from each tumor-bearing organ. In some experiments, mice were monitored routinely for weight loss, and survival times were used as the main criterion for determining treatment efficacy. All of the *in vivo* experiments have been performed at least three times with similar results.

Statistical Methods. The statistical significance of differential findings between experimental groups and controls was determined by Student's *t* test and considered significant if two-tailed *P*s were <0.05. Peto's log-rank test determined the significance of the differences between experimental groups in the survival experiments by the use of StatsDirect statistical software (CamCode, Ashwell, United Kingdom).

RESULTS

Characterization of NGR-Targeted Liposomes and Binding to Endothelial Cells *in Vitro*. Liposomes were typically 90–115 nm in diameter, with a DXR entrapment efficiency in liposomes of ~95%. All liposomal formulations showed minimal leakage in PBS, retaining >90% of the encapsulated DXR after a 24-h incubation. As expected from our previous data (28, 32), when leakage experiments were conducted in 25% human plasma, liposomes showed a slow DXR leakage (12%) at 24 h. For the targeting domain, we used the NGR motif, which binds a CD13 isoform selectively expressed by tumor-associated vessels (14, 29), for which there is evidence of internalization (6, 16). An average coupling efficiency for the NGR peptide of 55% (95% confidence interval = 50–60%) was obtained, resulting in a peptide density of 7–8 μg peptide/μmol PL.

To evaluate the specificity of NGR-SL[DXR], we used KS1767 cells, derived from Kaposi sarcoma because they bind the NGR-targeting peptide, as do endothelial cells (6, 16). The THP-1 (acute monocytic leukemia) cell line was used as a control because it does not bind the NGR peptide (14). FACS analysis showed that WM15 (a monoclonal antibody specific for CD13) bound to both THP-1 and KS1767 cells (Fig. 1, *A* and *D*, respectively). In contrast, NGR-SL[DXR] were able to bind the KS1767 cells (Fig. 1*E* and inset) but not the THP-1 cells (Fig. 1*B* and inset), thus confirming previous results indicating the existence of different isoforms within the CD13 molecule (14). Noteworthy, both WM-15 and NGR-SL[DXR] did not bind to SH-SY5Y NB cells (Fig. 1, *G* and *H*). To further confirm the selectivity of binding of our liposomal formulation, we used the mismatched peptide ARA as a targeting moiety. In this case, ARA-SL[DXR] did not bind to all cell lines (Fig. 1, *C*, *F*, and *I*).

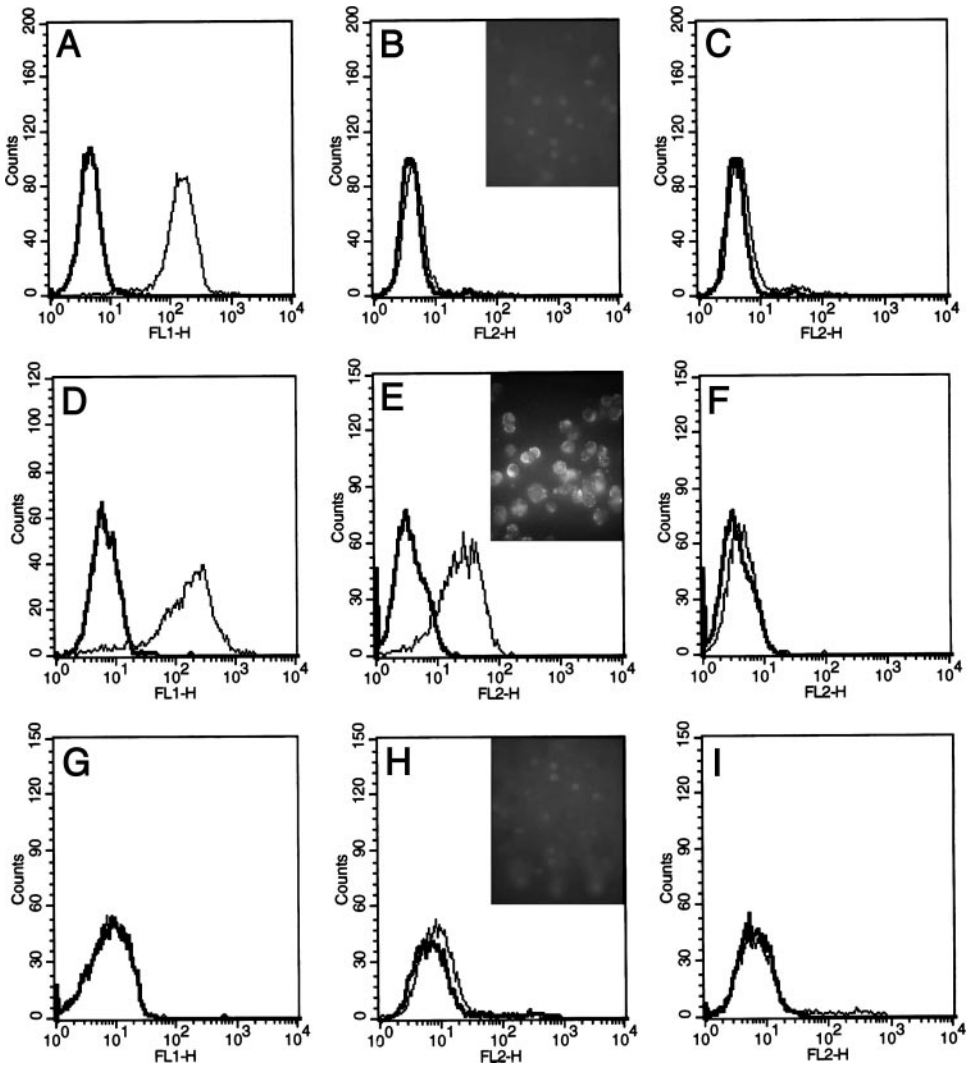

Fig. 1. Cellular association of NGR-targeted liposomes analyzed by flow cytometry. *A–C*, THP-1 cells; *D–F*, KS1767 cells; *G–I*, SH-SY5Y. Cells were incubated with WM15 monoclonal antibody (*a*, *d*, and *g*), NGR-SL[DXR]; (*B*, *E*, and *H*), or ARA-SL[DXR] (*C*, *F*, and *I*). After washing, cells treated with WM15 were incubated with a goat antimouse-FITC secondary antibody and then analyzed by FACS (*A*, *D*, and *G: thin lines*, WM15; *bold lines*, none). Cells treated with liposomal DXR were washed and directly enumerated by FACS (*B*, *C*, *E*, *F*, *H*, and *I: thin lines*, targeted liposomes; *bold lines*, nontargeted liposomes). In the insets *B*, *E*, and *H*, cells were evaluated for DXR fluorescence by fluorescence microscopy.

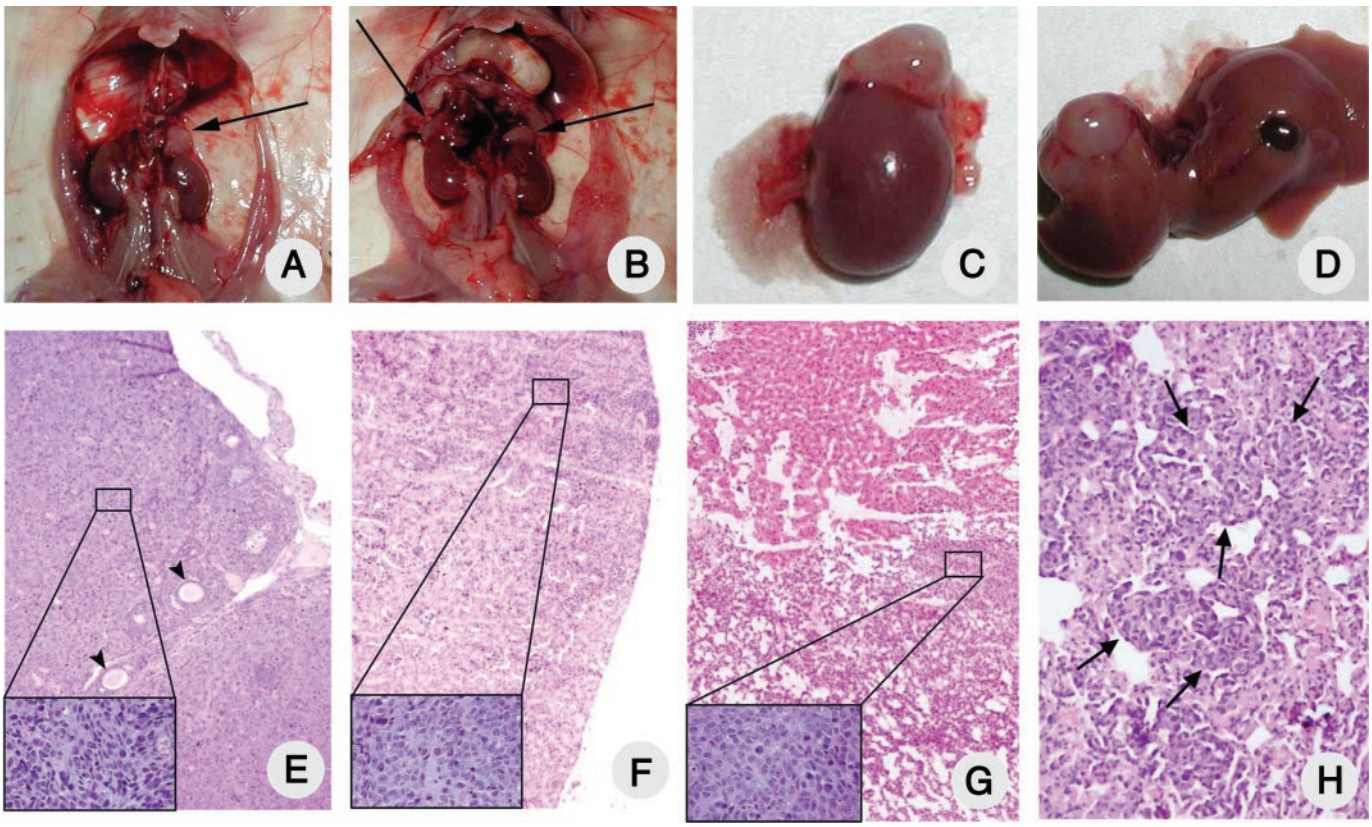

Fig. 2. Orthotopic NB xenograft model in SCID mice. *A* and *B*, adrenal gland tumors (*arrows*) in mice that were injected orthotopically with SH-SY5Y cells at 14 (*A*) and 21 (*B*) days before sacrifice. *C* and *D*, representative right adrenal gland (*C*) and liver (*D*) samples at 3 and 4 weeks after injection of NB cells, respectively. *E–H*, histological (H&E) analysis of representative ovary (*E*), kidney (*F*), liver (*G*), and lung (*H*) samples. Forty days after cell injection, animals were sacrificed, the organs were removed, fixed, paraffin embedded, sectioned at 5 μm, and stained with H&E. *Arrows* indicate metastatic tumor invasion in the lung. *Arrowheads* show the normal ovaric follicular structure surrounded by tumor NB cells. Magnification, ×10 (*insets*, ×63).

Biologically Relevant Orthotopic NB Xenograft Model. A more realistic view of the clinical potential of NGR-targeted liposomes could be obtained if a tumor model were available that better reflected the growth of advanced NB in children (*i.e.*, large adrenal gland tumors and multiple small metastatic lesions). All current data support this concept and recommend that orthotopic implantation of tumor cells in recipient animals is mandatory for studies of tumor progression, angiogenesis, invasion, and metastasis (33).

To provide a well-characterized, relevant, highly reproducible, angiogenic, and metastatic orthotopic model of NB, we initiated studies to define five adrenal NB xenograft models based on previously described human NB cell lines (30) and reported animal models (34, 35). From these data (data not shown), we decided to use the intra-adrenal injection of SH-SY5Y cells in mice for additional studies because, 2–3 weeks after injection, adrenal gland tumors were always found in all animals (Fig. 2*A*). This model best reflected the typical growth pattern of human NB because orthotopic injection of SH-SY5Y cells resulted in solid adrenal tumors that were highly vascular, locally invasive into surrounding tissues, and metastatic to distant sites. Indeed, macroscopic metastases always occurred after 3–4 weeks of injection in the contralateral adrenal (Fig. 2, *B* and *C*) and liver (Fig. 2*D*), whereas micrometastases were apparent frequently in the ovary (Fig. 2*E*), right kidney (Fig. 2*F*), liver (Fig. 2*G*), and lung (Fig. 2*H*).

PK and BD Profiles of NGR-Targeted Liposomes. As previously shown (36), long circulation times are required for SLs to gain access to tumor sites. Thus, the PKs and BD of [^{3}H]CHE-labeled SL[DXR] and NGR-SL[DXR] was evaluated in xenograft models of orthotopic NB in SCID mice. The results of the PK studies are expressed as percentage of the administered dose of lipid remaining in blood. These findings clearly indicate that liposomes coupled to NGR peptide had long-circulating profiles in blood, being almost identical to that obtained with nontargeted SL[DXR] (Fig. 3*A*). The BD of liposomes was evaluated at 2, 12, and 24 h after injection. At all times, the spleen uptake of targeted liposomes was ~10–20 times higher than that of SL. No differences between uptake of SL[DXR] *versus* NGR-SL[DXR] occurred in other tissues, and with the exception of liver, uptake into other organs was very low (Table 1). Finally, we evaluated the tumor accumulation of targeted and nontargeted liposomes. The uptake into tumor by NGR-SL[DXR] was time dependent, being at least 10 times higher than that of SL[DXR] after 24 h (Fig. 3*B*). No uptake was observed into tumors of mice treated with ARA-SL[DXR]; (Fig. 3, *B* and *F*).

Homing to Tumor Vasculature. To determine whether the NGR-targeted liposomes could deliver DXR to angiogenic tumor-associated blood vessels, we injected NGR-SL[DXR] into the tail vein of mice bearing established adrenal tumors. In one set of experiments, liposomes were allowed to circulate from 2 to 24 h, followed by perfusion and immediate tissue recovery. There was a clear time-dependent uptake of DXR in the tumor vasculature (Fig. 3, *C–E*). At 24 h, the staining pattern indicated that the DXR had spread outside the blood vessels and into the tumors. This spreading may be attributable to increased permeability of tumor blood vessels to the intact liposomes (37) or uptake of the targeted liposomes by angiogenic endothelial cells and subsequent transfer to tumor cells, as shown for the uptake of phage (6). Likely, both mechanisms are working at the same time. In the second set of experiments, tissues were examined 16 h after the injection of NGR-SL[DXR] or ARA-SL[DXR]. Strong DXR staining

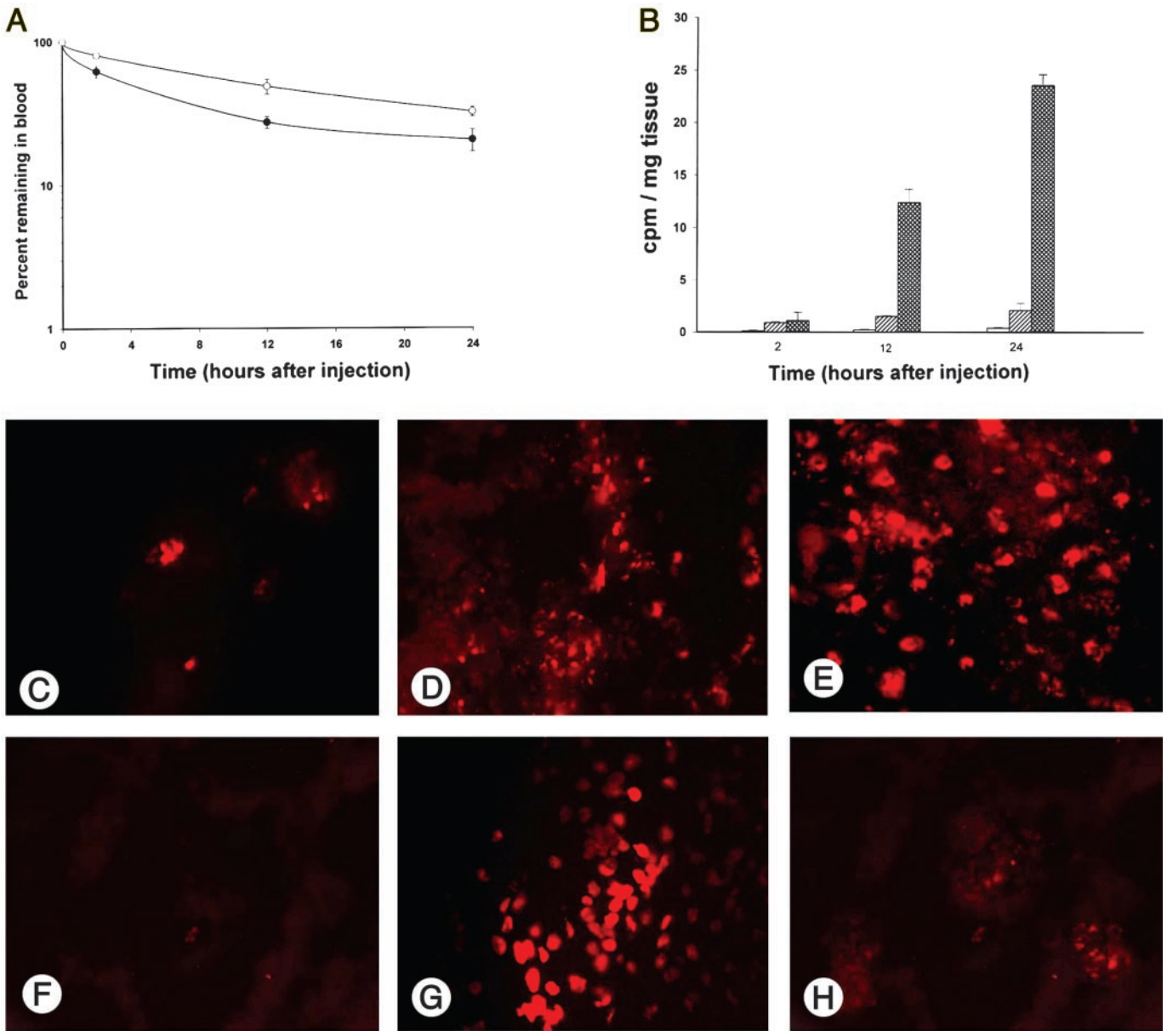

Fig. 3. *A*, blood clearance kinetics of nontargeted and NGR-targeted DXR-loaded liposomes in SCID mice. Liposomes were labeled with the lipid tracer [^{3}H]CHE and were administered i.v. in a single bolus dose (0.5 μmol PL/mouse). Treatment groups consisted of NGR-SL[DXR]; (●) and SL[DXR]; (○). At different times after injection, blood was collected and counted for [^{3}H] label. Each point represents the average of three mice ± SD. *B*, tumor accumulation of NGR-targeted DXR-loaded liposomes in SCID mice injected orthotopically with NB cells. [^{3}H]-labeled DXR-loaded liposomes, either nontargeted (▨), ARA-targeted (□), or NGR-targeted (▩) were injected via the tail vein as a single bolus dose. After 2, 12, and 24 h, tumors were collected and counted for [^{3}H] label. Results are expressed as cpm/mg tissue. Each point represents the average of three mice (±SD). *C–H*, tumor accumulation of NGR-targeted liposomal DXR. Mice were treated with NGR-SL(DXR) as in *B*. After 2 (*C*), 12 (*D*), and 24 (*E*) h, tumors were collected and DXR visualized by fluorescence microscopy of fixed, paraffin-embedded, tissue sections. Alternatively, mice were injected with control ARA-SL[DXR]; (*F*), with NGR-SL[DXR] either alone (*G*) or coinjected with a 50-fold excess of the soluble NGR peptide (*H*) and tumors collected after 16 h. Magnitude, ×40.

in tumor vasculature was seen only in animals treated with NGR-liposomes (Fig. 3, *G versus F*). At this time, minimal DXR staining was observed in the spleen and liver, and no detectable expression was found in the heart, lung, kidney, and brain (data not shown). Tumor-specific DXR uptake was completely blocked when mice were coinjected with a 50-fold molar excess of the soluble NGR peptide (Fig. 3*H*).

***In Vivo* Therapeutic Studies.** To determine whether liposomes homing to the tumor vasculature could be used to improve the therapeutic index of the chemotherapeutic agent DXR, we injected SH-SY5Y cells into the left adrenal gland of SCID mice and allowed them to grow for 21 days, at which time, they reached a size of ~200 mm^3. The commonly used dose of DXR in SCID mice with human tumor xenografts is 1–3 mg/kg/week for 3–4 weeks (38, 39). Because we expected the liposomal DXR to be more effective and less toxic than the free drug, we initially performed a dose-escalation experiment in which mice with established tumors were treated with different doses of DXR once a week for 3 weeks and then observed for an extended period of time. Tumor-bearing mice treated with 2 mg/kg/week outlived the control mice, all of which died from widespread disease (Fig. 4*A*, log-rank test, $P < 0.001$ and Fig. 4, *B–D*). However, higher doses were toxic because all of the mice treated with 4 and 8 mg/kg/week died within 48 h of the third and second drug administration, respectively. Thus, the maximum-tolerated dose of targeted liposomal DXR in SCID mice was between 6 and 12 mg.

To assess the impact of NGR-SL[DXR] on tumor cell viability, we

Table 1 *Tissue distributions of NGR-targeted or nontargeted liposomes in SCID mice*

	Lung	Heart	Spleen	Liver	Kidney	Brain
Time	% of injected dose					
NGR-^{3}H-SL[DXR]						
2 h	1.28 ± 0.63	0.00	25.90 ± 5.07	11.11 ± 4.19	0.38 ± 0.03	0.00
12 h	0.91 ± 0.11	0.01 ± 0.01	48.42 ± 0.12	23.52 ± 2.18	0.43 ± 0.10	0.00
24 h	0.86 ± 0.12	0.05 ± 0.03	55.43 ± 3.18	22.41 ± 5.92	0.68 ± 0.12	0.00
^{3}H-SL[DXR]						
2 h	0.12 ± 0.01	0.02 ± 0.03	0.32 ± 0.26	3.96 ± 1.84	0.90 ± 0.17	0.00
12 h	0.09 ± 0.01	0.03 ± 0.01	2.64 ± 0.15	22.78 ± 0.62	1.10 ± 0.96	0.00
24 h	0.08 ± 0.01	0.12 ± 0.06	4.15 ± 0.26	29.25 ± 0.99	1.91 ± 0.4	0.00

stained cryosections taken from tumors at 24 h after the third treatment and examined them at low and medium magnification to evaluate both blood vessels and surrounding tumor parenchyma. Histopathological analysis of excised tumor on day 36 revealed pronounced destruction of the tumor vasculature with a marked decreased in vessel density after treatment of the mice with 2 mg/kg/week × 3 of NGR-SL[DXR]; (Fig. 4*G*). Double staining of tumors with TUNEL and antifactor VIII antibody or antihuman NB, demonstrated endothelial cell apoptosis in the vasculature (Fig. 4*I*), as well as increased tumor cell apoptosis (Fig. 4*M*), respectively. Interestingly, apoptosis induced by NGR-SL[DXR] was prominent only in the tumor tissues; similar treatment resulted in no observable apoptosis in normal tissue such as heart, lung, kidneys, liver, and spleen (data not shown).

To further test the therapeutic efficacy of this treatment, we randomly sorted mice bearing established 200 mm^3 of SH-SY5Y adrenal tumors into three groups and treated each group with a weekly tail vein injection of HEPES buffer (untreated controls) or 3 mg/kg DXR entrapped in NGR-SL or in ARA-SL for 3 consecutive weeks. Mice injected with HEPES buffer or ARA-SL[DXR] or NGR-SL without DXR (data not shown) formed large tumors (1100–1200 mm^3) and, consequently, were euthanized on day 42 (Fig. 5*A*). In contrast, mice injected with NGR-SL[DXR] displayed rapid tumor regression (Fig. 5*A*). One day after the third treatment, four of six mice showed no evidence of tumors, and the two others showed a >80% reduction in tumor mass and a >90% suppression of blood vessel density (Fig. 5*A* inset; $P < 0.01$). These findings demonstrated that aminopeptidase N-targeting delivery of DXR to blood vessels caused tumor regression because of its ability to promote apoptosis of the angiogenic endothelium.

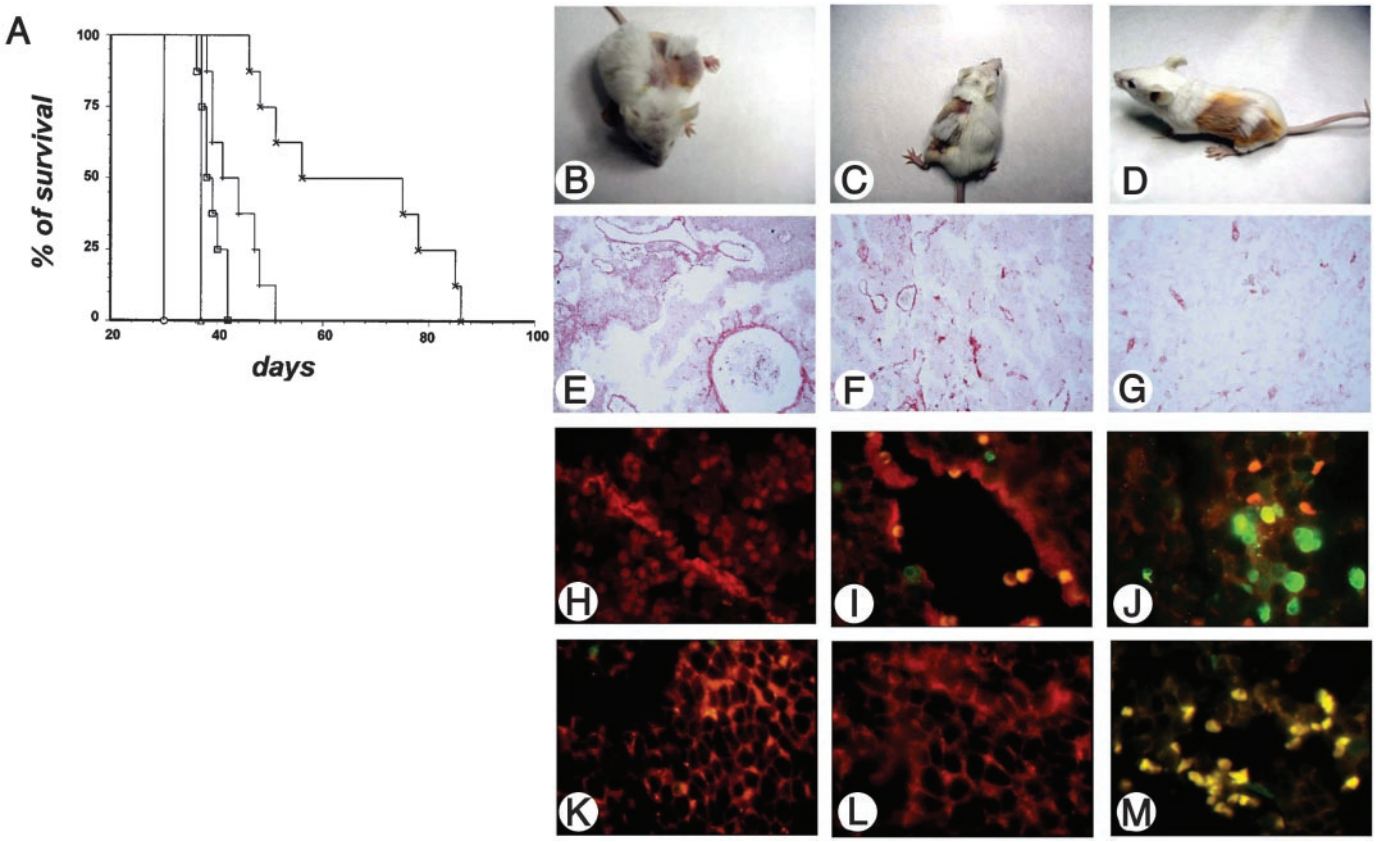

Fig. 4. Antitumor effects of NGR-targeted liposomal DXR *in vivo*. *A*, dose-dependent effects of NGR-SL[DXR] on the survival of tumor-bearing mice. Treatment groups (n = 8/group) consisted of HEPES buffer (control, □), NGR-SL[DXR] at 8 mg/kg (○), 4 mg/kg (△), 2 mg/kg (×), and 1 mg/kg (+). Mice received injections in the adrenal gland with SH-SY5Y cells on day 0 and received the various treatments 21, 28, and 35 days after inoculation. *B–D*, mice were inoculated and treated as in *a*, then photographed on day 36: *B*, control; *C*, treated with 1 mg/kg/week; *D*, treated with 2 mg/kg/week. *E–M*, IHC analysis. Tumors were harvested on day 36 from control mice (*E*, *H*, and *K*) and mice treated with 1 mg/kg/week (*F*, *I*, and *L*) or 2 mg/kg/week (*G*, *J*, and *M*) as in *A*. Tissue sections were immunostained for the expression of factor VIII (to show vessels, *E*, *F*, and *G*; magnitude ×10) or for a double label of factor VIII (endothelial cells) and TUNEL (apoptosis; *H*, *I*, and *J*) or for a double label of NB84a (NB cells) and TUNEL (*K*, *L*, and *M*). *Red*, factor VIII+ endothelial cells or NB84a+ NB cells; *green*, TUNEL+ cells; *yellow*, colocalization of TUNEL+-factor VIII+ or –NB84a+ cells. *H–M*, ×40 magnification.

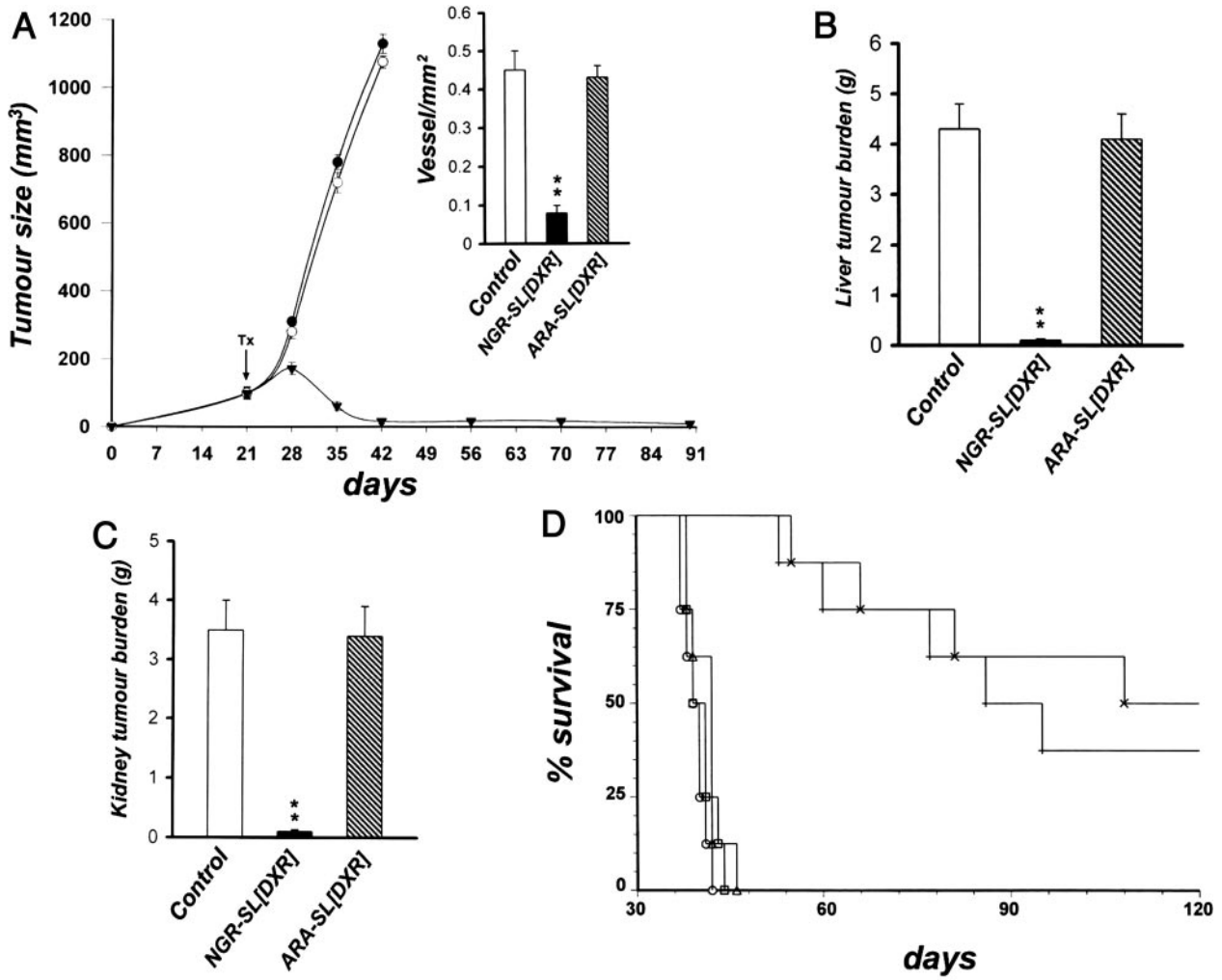

Fig. 5. Delivery of DXR to tumor vessels inhibits angiogenesis, causing regression of established NB tumors. *A*, SCID mice orthotopically implanted in the left adrenal gland with NB cells were allowed to form tumors of ~200 mm^3 in size and were then injected i.v. with 3 mg DXR/kg/week as in Fig. 4. Tx, start of treatment. (●) HEPES buffer control; (○) ARA-SL[DXR]; (▲) NGR-SL[DXR]. Each point represents the mean ± SD of six replicates. *Inset*, orthotopic tumors, at day 36 from control and DXR-treated groups, were sectioned and stained with an antibody to factor VIII to count blood vessels. Each *bar* represents the mean ± SD of five replicates. *B* and *C*, mice were treated as above, and on day 36, organs (liver, *B*; kidney, *C*) were harvested and weighed. Each *bar* represents the mean ± SD of six mice. (**,--) $P < 0.01$). *D*, effects of different schedules of treatment with NGR-SL[DXR] on life span. Treatment groups ($n = 8$/group) consisted of HEPES buffer (control, □); free DXR (△) or NGR-SL[DXR]; (+), treated with 3 mg/kg on days 21, 28, and 35; free DXR (○) or NGR-SL[DXR; ×] treated with 1 mg/kg every other 2 days starting on day 21 for a total of nine injections.

We next examined whether this therapy was also effective against established metastases. Control mice treated with HEPES buffer or ARA-SL[DXR] showed extensive tumor burdens in the liver and right kidney (Fig. 5, *B* and *C*). In contrast, mice treated with NGR-SL[DXR] displayed little or no visible tumor metastasis, as demonstrated by a significant reduction in wet liver or kidney weight (Fig. 5, *B* and *C*; $P < 0.01$).

Finally, to test whether continuous low-dose administration of chemotherapy agents or antiangiogenic schedule chemotherapy (19, 20) could also inhibit orthotopically placed NB tumors, we compared our standard dosing schedule of 3 mg/kg/wk × 3 with a metronomic administration of DXR, either free or encapsulated into NGR-targeted liposomes (1 mg/kg/every other 2 days × 9). Complete tumor eradication was seen in all animals treated with either schedule. However, the observed tumor growth inhibition was maintained beyond 4 months in four of eight mice and in three of eight mice treated with the metronomic or the standard schedule, respectively, showing a significant improvement ($P < 0.0001$ and $P = 0.0002$, respectively) in long-term survival compared with control animals or mice treated with free DXR (Fig. 5*D*).

DISCUSSION

We have developed a novel targeting strategy that might overcome problems of tumor cell heterogeneity. We accomplished this by using targeted liposomes to exploit the obvious advantages of anti-angiogenic therapies developed by many other investigators (4, 19, 20, 40, 41). We have shown that pronounced tumor regressions can be achieved in mice by systemic delivery a liposomal anti-angiogenic chemotherapeutic drug that is targeted to the tumor vasculature. There are several advantages of targeting chemotherapeutic agents to proliferating endothelial cells in the tumor vasculature rather than directly to tumor cells. First, acquired drug resistance resulting from genetic and epigenetic mechanisms reduces the effectiveness of available drugs (19, 20). Anti-angiogenic therapy has the potential to overcome these problems or reduce their impact. This therapy targets the tumor vasculature, derived from local and circulating endothelial cells, that are considered genetically stable. Second, the fact that many cancer cells depend upon a few endothelial cells for their growth and survival might also amplify the therapeutic effect (42). Third, anti-angiogenic therapies may also circumvent what may be a major mechanism of

intrinsic drug resistance, namely insufficient drug penetration into the interior of a tumor mass because of high interstitial pressure gradients within tumors (43). A strategy that targets both the tumor vasculature and the tumor cells themselves may be more effective than strategies that target only tumor vasculature because this strategy can leave a cuff of unaffected tumor cells at the tumor periphery that can subsequently regrow and kill the animals (44). Fourth, oxygen consumption by neoplastic and endothelial cells, along with poor oxygen delivery, creates hypoxia within tumors. These pathophysiological characteristics of solid tumors compromise the delivery and effectiveness of conventional cytotoxic therapies, as well as molecularly targeted therapies (42, 43). Finally, the therapeutic target is independent of the type of solid tumor; killing of proliferating endothelial cells in the tumor microenvironment can be effective against a variety of malignancies.

Most deaths from cancer are because of metastases that are resistant to conventional therapies. One of the most relevant principles of anticancer therapy design is that the outcome of metastases depends on multiple interactions of metastatic cells with homeostatic mechanisms (45). Therapy of metastasis, therefore, could be targeted not only against tumor cells but also against the homeostatic factors that are favorable to the growth and survival of metastatic cells. The targeting of therapies to the vasculature of tumors overcomes some of the problems of conventional tumor targeting.

Vascular targeting exploits molecular differences that exist in blood vessels of different organs and tissues, as well as differences between normal blood vessels and angiogenic tumor vessels. Differences in plasma membrane proteins (vascular zip codes) can be used to target therapeutic or imaging agents directly to a particular organ or tumor (2, 3). Many studies have now documented the specialization of the vasculature in tumors, both with respect to structural abnormalities and to potential molecular targets (1, 2). *In vivo* phage display is leading to the identification of peptides that home to tumor vessels, and such tumor-homing peptides can target therapies to tumors (6, 9, 15, 16).

Here, we developed an antitumor therapeutic strategy based on selective expression of vascular receptors in tumors. Previous studies showed that NGR-containing peptides bind to an aminopeptidase N isoform expressed in tumor vessels and not other isoforms expressed in normal epithelia or myeloid cells (14). Because liposomes are effective drug delivery systems and their physicochemical features can be manipulated with relative ease (11), tumor vessel-specific liposomes would be an effective strategy for delivery of cytotoxic drugs not only to tumor endothelial cells but also directly to tumor cells themselves via the passive targeting phenomenon (11). One of the primary goals of a successful cancer treatment regimen is to deliver sufficient amounts of drug to tumors while minimizing damage to healthy surrounding tissues. Cationic liposomes have been shown to associate directly with the endothelium of tumor vessels (46, 47). However, several lines of evidence now suggest that drug-associated cationic liposomal formulations may result in clinical complications. The vascular network is a highly accessible target for tumor therapy, but to be successful, an antivascular strategy should target as many tumor vessels as possible. We reasoned that the multivalent display of specific peptides at the surface of neutral liposomes could be more effective in active targeting of the tumor vasculature than cationic liposomes. By coupling NGR peptide to the polyethylene glycol terminus of sterically stabilized liposomes, we have taken the first step toward optimizing liposome-based delivery to improve the next generation of vasculature-targeted therapeutics. The high targeting efficiency observed *in vitro* and *in vivo* of NGR-targeted liposomes, taken together with the lack of binding and activity of the ARA-targeted liposomal formulation, clearly indicated a pivotal role of the NGR receptor in tumor angiogenesis (7, 13). Because the NGR receptor is an internalizing epitope (6), our data support the hypothesis that after binding and internalization of the liposomal drug packages, the breakdown of the drug-liposome package by lysosomal and endosomal enzymes and release of drug into the endothelial cell interior are responsible for the cytotoxic effects produced by targeted liposomal DXR (32). Internalization of antibodies or other ligands into the target cells is also required for other targeted therapeutics such as immunotoxins and antibody-drug conjugates and for targeted delivery of genes or viral DNA into cells (11, 12).

The molecular mechanisms underlying the selective interaction of NGR-targeted liposomal DXR with tumor vasculature have been partially elucidated. We have recently shown that different CD13 isoforms exist and that the NGR domain recognize selectively a CD13 isoform associated with tumor vessels (14). We hypothesize, therefore, that NGR-targeted liposomes rapidly interact with CD13-positive endothelial cells because of high-avidity multivalent binding and that they interact little or not at all with CD13-negative endothelial cells of normal vessels because of lower avidity, confirming our previous finding obtained with the construct NGR-tumor necrosis factor (7). In this study, we found that treatment with NGR-targeted liposomal formulations of DXR inhibited vascularization and, hence, reduced total tumor volume and weight. IHC analysis of the orthotopic NB tumors demonstrated a significant decrease in microvessel density with an associated increase in apoptosis of tumor cells and tumor-associated endothelial cells. Indeed, double staining of endothelial cells with antibodies against factor VIII and TUNEL suggested that the reduction in microvessel density was attributable to a pronounced increase of apoptosis in the endothelial cells.

Most preclinical studies on tumor angiogenesis and antiangiogenic therapy usually use rapidly growing transplantable mouse tumors or human tumor xenografts, which are grown as solid, localized tumors in the s.c. space. For several reasons, this approach almost certainly exaggerates the antitumor responses. Principally, in such experimental situations, unlike in the clinic, distant metastases are usually not the focus of the treatment, but it is precisely such secondary tumors that are ultimately responsible for cancer's lethality. For these reasons and to elucidate possible influences of the host microenvironment, we decided to carry out angiogenesis-specific studies of tumors in an orthotopic location. The use of orthotopically transplanted NB tumors may be preferable for these studies, not only to induce or enhance the incidence of metastases but also because the response of a tumor mass growing ectopically may be abnormal compared with the same tumor growing in a physiologically relevant site (45). The convincing anti-angiogenic effects of NGR-targeted liposomal DXR in our earlier studies led us to test this drug formulation for antitumor effects in this clinically relevant situation. The potency of the targeted DXR formulation in this tumor model was revealed by its ability to control and effectively shrink established orthotopic NB tumors in mice. The hypothesis that NGR-SL[DXR] affects tumor growth primarily through anti-angiogenesis is supported by our data showing fewer factor VIII-positive blood vessels in orthotopic tumors treated with NGR-SL[DXR] compared with control tumors. The theory is additionally supported by our observation of an atypical dose response effect on established tumors. Indeed, a relatively low, noncytotoxic dose of NGR-SL[DXR], when frequently administered, caused the tumor to regress. This observation is consistent with the low dose delayed effects on tumors typically seen with other reported antiangiogenic treatment protocols (19, 20). Low-dose anti-angiogenic therapy is currently being explored as an antitumor experimental therapy (18). In our orthotopic NB model, we clearly showed that targeting the

chemotherapeutic agent DXR to tumor vessels makes it possible to combine blood vessel destruction with the conventional antitumor actions of drug. Our findings are in agreement with previous results showing that in mice bearing human cancer xenografts, an anti-angiogenic approach has proven more efficacious and less toxic than conventional therapy (6, 15, 16, 39). However the targeted liposome approach may have another advantage because, in our studies, liposomal DXR appeared to escape from the vasculature and be delivered directly to the tumor interstitial space. Delivery of liposomal DXR to tumors by passive targeting (because the NGR-targeted liposomes are not expected to bind to tumor cells directly) is the mechanism of action of the successful clinical liposomal drug, Doxil/Caelyx (48). This potential for dual action of the NGR-targeted liposomes may result in a higher and more durable anticancer effect than a strictly antiangiogenic approach.

Although our studies have been performed in a mouse model, we expect the NGR motif to target human vasculature as well because the NGR phage has been shown to bind to blood vessels of human tumors (6). Thus, this peptide is potentially suitable for tumor targeting in patients.

In conclusion, the targeting of the vasculature of diseased organs could be the basis of a new pharmacological approach for the treatment of malignancies by taking advantage of formulations that delivery cytotoxic drugs to both blood vessels located specifically at sites of disease and to the tumor cells themselves. This should improve efficacy and reduce side effects.

ACKNOWLEDGMENTS

We thank F. Comanducci and L. Tedeschi for expert technical assistance, P. G. Montaldo, M. V. Corrias, G. Pagnan and V. Pistoia for helpful discussions, and C. Bernardini for editing.

REFERENCES

1. Kolonin, M., Pasqualini, R., and Arap, W. Molecular addresses in blood vessels as targets for therapy. Curr. Opin. Chem. Biol., *5:* 308–313, 2001.
2. Trepel, M., Arap, W., and Pasqualini, R. *In vivo* phage display and vascular heterogeneity: implications for targeted medicine. Curr. Opin. Chem. Biol., *6:* 399–404, 2002.
3. Arap, W., Kolonin, M. G., Trepel, M., Lahdenranta, J., Cardo-Vila, M., Giordano, R. J., Mintz, P. J., Ardelt, P. U., Yao, V. J., Vidal, C. I., Chen, L., Flamm, A., Valtanen, H., Weavind, L. M., Hicks, M. E., Pollock, R. E., Botz, G. H., Bucana, C. D., Koivunen, E., Cahill, D., Troncoso, P., Baggerly, K. A., Pentz, R. D., Do, K. A., Logothetis, C. J., and Pasqualini, R. Steps toward mapping the human vasculature by phage display. Nat. Med., *8:* 121–127, 2002.
4. Folkman, J. Angiogenesis in cancer, vascular, rheumatoid and other disease. Nat. Med., *1:* 27–31, 1995.
5. Boehm, T., Folkman, J., Browder, T., and O'Reilly, M. S. Antiangiogenic therapy of experimental cancer does not induce acquired drug resistance. Nature (Lond.), *390:* 404–407, 1997.
6. Arap, W., Pasqualini, R., and Ruoslahti, E. Cancer treatment by targeted drug delivery to tumor vasculature in a mouse model. Science (Wash. DC), *279:* 377–380, 1998.
7. Curnis, F., Sacchi, A., and Corti, A. Improving chemotherapeutic drug penetration in tumors by vascular targeting and barrier alteration. J. Clin. Investig., *110:* 475–482, 2002.
8. Sipkins, D. A., Cheresh, D. A., Kazemi, M. R., Nevin, L. M., Bednarski, M. D., and Li, K. C. Detection of tumor angiogenesis *in vivo* by $\alpha V\beta 3$-targeted magnetic resonance imaging. Nat. Med., *4:* 623–626, 1998.
9. Hood, J. D., Bednarski, M., Frausto, R., Guccione, S., Reisfeld, R. A., Xiang, R., and Cheresh, D. A. Tumor regression by targeted gene delivery to the neovasculature. Science (Wash. DC), *296:* 2404–2407, 2002.
10. Niethammer, A. G., Xiang, R., Becker, J. C., Wodrich, H., Pertl, U., Karsten, G., Eliceiri, B. P., and Reisfeld, R. A. A DNA vaccine against VEGF receptor 2 prevents effective angiogenesis and inhibits tumor growth. Nat. Med., *8:* 1369–1375, 2002.
11. Allen, T. M. Ligand-targeted therapeutics in anticancer therapy. Nat. Rev. Cancer, *2:* 750–763, 2002.
12. Sapra, P., and Allen, T. M. Internalizing antibodies are necessary for improved therapeutic efficacy of antibody-targeted liposomal drugs. Cancer Res., *62:* 7190–7194, 2002.
13. Pasqualini, R., Koivunen, E., Kain, R., Lahdenranta, J., Sakamoto, M., Stryhn, A., Ashmun, R. A., Shapiro, L. H., Arap, W., and Ruoslahti, E. Aminopeptidase N is a receptor for tumor-homing peptides and a target for inhibiting angiogenesis. Cancer Res., *60:* 722–727, 2000.
14. Curnis, F., Arrigoni, G., Sacchi, A., Fischetti, L., Arap, W., Pasqualini, R., and Corti, A. Differential binding of drugs containing the NGR motif to CD13 isoforms in tumor vessels, epithelia, and myeloid cells. Cancer Res., *62:* 867–874, 2002.
15. Curnis, F., Sacchi, A., Borgna, L., Magni, F., Gasparri, A., and Corti, A. Enhancement of tumor necrosis factor α antitumor immunotherapeutic properties by targeted delivery to aminopeptidase N (CD13). Nat. Biotechnol., *18:* 1185–1190, 2000.
16. Ellerby, H. M., Arap, W., Ellerby, L. M., Kain, R., Andrusiak, R., Rio, G. D., Krajewski, S., Lombardo, C. R., Rao, R., Ruoslahti, E., Bredesen, D. E., and Pasqualini, R. Anti-cancer activity of targeted pro-apoptotic peptides. Nat. Med., *5:* 1032–1038, 1999.
17. Bocci, G., Nicolaou, K. C., and Kerbel, R. S. Protracted low-dose effects on human endothelial cell proliferation and survival *in vitro* reveal a selective antiangiogenic window for various chemotherapeutic drugs. Cancer Res., *62:* 6938–6943, 2002.
18. Miller, K. D., Sweeney, C. J., and Sledge, G. W., Jr. Redefining the target: chemotherapeutics as antiangiogenics. J. Clin. Oncol., *19:* 1195–1206, 2001.
19. Browder, T., Butterfield, C. E., Kraling, B. M., Shi, B., Marshall, B., O'Reilly, M. S., and Folkman, J. Antiangiogenic scheduling of chemotherapy improves efficacy against experimental drug-resistant cancer. Cancer Res., *60:* 1878–1886, 2000.
20. Klement, G., Baruchel, S., Rak, J., Man, S., Clark, K., Hicklin, D. J., Bohlen, P., and Kerbel, R. S. Continuous low-dose therapy with vinblastine and VEGF receptor-2 antibody induces sustained tumor regression without overt toxicity. J. Clin. Investig., *105:* R15–R24, 2000.
21. Hanahan, D., Bergers, G., and Bergsland, E. Less is more, regularly: metronomic dosing of cytotoxic drugs can target tumor angiogenesis in mice. J. Clin. Investig., *105:* 1045–1047, 2000.
22. Gately, S., and Kerbel, R. Antiangiogenic scheduling of lower dose cancer chemotherapy. Cancer J, *7:* 427–436, 2001.
23. Maris, J. M., and Matthay, K. K. Molecular biology of neuroblastoma. J. Clin. Oncol., *17:* 2264–2279, 1999.
24. Meitar, D., Crawford, S. E., Rademaker, A. W., and Cohn, S. L. Tumor angiogenesis correlates with metastatic disease, N-myc amplification, and poor outcome in human neuroblastoma. J. Clin. Oncol., *14:* 405–414, 1996.
25. Sugiura, Y., Shimada, H., Seeger, R. C., Laug, W. E., and DeClerck, Y. A. Matrix metalloproteinases-2 and -9 are expressed in human neuroblastoma: contribution of stromal cells to their production and correlation with metastasis. Cancer Res., *58:* 2209–2216, 1998.
26. Ribatti, D., Surico, G., Vacca, A., De Leonardis, F., Lastilla, G., Montaldo, P. G., Rigillo, N., and Ponzoni, M. Angiogenesis extent and expression of matrix metalloproteinase-2 and -9 correlate with progression in human neuroblastoma. Life Sci., *68:* 1161–1168, 2001.
27. Ribatti, D., Alessandri, G., Vacca, A., Iurlaro, M., and Ponzoni, M. Human neuroblastoma cells produce extracellular matrix-degrading enzymes, induce endothelial cell proliferation and are angiogenic *in vivo*. Int. J. Cancer, *77:* 449–454, 1998.
28. Pastorino, F., Brignole, C., Marimpietri, D., Sapra, P., Moase, E. H., Allen, T. M., and Ponzoni, M. Doxorubicin-loaded Fab′ fragments of anti-disialoganglioside immunoliposomes selectively inhibit the growth and dissemination of human neuroblastoma in nude mice. Cancer Res., *63:* 86–92, 2003.
29. Colombo, G., Curnis, F., De Mori, G. M., Gasparri, A., Longoni, C., Sacchi, A., Longhi, R., and Corti, A. Structure-activity relationships of linear and cyclic peptides containing the NGR tumor-homing motif. J. Biol. Chem., *277:* 47891–47897, 2002.
30. Ponzoni, M., Bocca, P., Chiesa, V., Decensi, A., Pistoia, V., Raffaghello, L., Rozzo, C., and Montaldo, P. G. Differential effects of *N*-(4-hydroxyphenyl)retinamide and retinoic acid on neuroblastoma cells: apoptosis versus differentiation. Cancer Res., *55:* 853–861, 1995.
31. Moreira, J. N., Hansen, C. B., Gaspar, R., and Allen, T. M. A growth factor antagonist as a targeting agent for sterically stabilized liposomes in human small cell lung cancer. Biochim. Biophys. Acta, *1514:* 303–317, 2001.
32. Lopez De Mendez, D. E., Kirchmeier, M. J., Gagne, J. F., Pilarski, L. M., and Allen, T. M. Cellular trafficking and cytotoxicity of anti-CD19-targeted liposomal doxorubicin in B lymphoma cells. J. Liposome Res., *9:* 199–228, 1999.
33. Chambers, A. F., Groom, A. C., and MacDonald, I. C. Dissemination and growth of cancer cells in metastatic sites. Nat. Rev. Cancer, *2:* 563–572, 2002.
34. Engler, S., Thiel, C., Forster, K., David, K., Bredehorst, R., and Juhl, H. A novel metastatic animal model reflecting the clinical appearance of human neuroblastoma: growth arrest of orthotopic tumors by natural, cytotoxic human immunoglobulin M antibodies. Cancer Res., *61:* 2968–2973, 2001.
35. Khanna, C., Jaboin, J. J., Drakos, E., Tsokos, M., and Thiele, C. J. Biologically relevant orthotopic neuroblastoma xenograft models: primary adrenal tumor growth and spontaneous distant metastasis. In Vivo, *16:* 77–85, 2002.
36. Gabizon, A., Catane, R., Uziely, B., Kaufman, B., Safra, T., Cohen, R., Martin, F., Huang, A., and Barenholz, Y. Prolonged circulation time and enhanced accumulation in malignant exudates of doxorubicin encapsulated in polyethylene-glycol coated liposomes. Cancer Res., *54:* 987–992, 1994.
37. Jain, R. K. Delivery of molecular medicine to solid tumors. Science (Wash. DC), *271:* 1079–1080, 1996.
38. Moase, E. H., Qi, W., Ishida, T., Gabos, Z., Longenecker, B. M., Zimmermann, G. L., Ding, L., Krantz, M., and Allen, T. M. Anti-MUC-1 immunoliposomal doxorubicin in the treatment of murine models of metastatic breast cancer. Biochim. Biophys. Acta, *1510:* 43–55, 2001.
39. Zhang, L., Yu, D., Hicklin, D. J., Hannay, J. A., Ellis, L. M., and Pollock, R. E. Combined anti-fetal liver kinase 1 monoclonal antibody and continuous low-dose doxorubicin inhibits angiogenesis and growth of human soft tissue sarcoma xenografts by induction of endothelial cell apoptosis. Cancer Res., *62:* 2034–2042, 2002.

40. O'Reilly, M. S., Holmgren, L., Chen, C., and Folkman, J. Angiostatin induces and sustains dormancy of human primary tumors in mice. Nat. Med., *2:* 689–692, 1996.
41. O'Reilly, M. S., Boehm, T., Shing, Y., Fukai, N., Vasios, G., Lane, W. S., Flynn, E., Birkhead, J. R., Olsen, B. R., and Folkman, J. Endostatin: an endogenous inhibitor of angiogenesis and tumor growth. Cell, *88:* 277–285, 1997.
42. Jain, R. K. Normalizing tumor vasculature with anti-angiogenic therapy: a new paradigm for combination therapy. Nat. Med., *7:* 987–989, 2001.
43. Jain, R. K. The next frontier of molecular medicine: delivery of therapeutics. Nat. Med., *4:* 655–657, 1998.
44. Huang, X., Molema, G., King, S., Watkins, L., Edgington, T. S., and Thorpe, P. E. Tumor infarction in mice by antibody-directed targeting of tissue factor to tumor vasculature. Science (Wash. DC), *275:* 547–550, 1997.
45. Fidler, I. J. Modulation of the organ microenvironment for treatment of cancer metastasis. J. Natl. Cancer Inst. (Bethesda), *87:* 1588–1592, 1995.
46. Campbell, R. B., Fukumura, D., Brown, E. B., Mazzola, L. M., Izumi, Y., Jain, R. K., Torchilin, V. P., and Munn, L. L. Cationic charge determines the distribution of liposomes between the vascular and extravascular compartments of tumors. Cancer Res., *62:* 6831–6836, 2002.
47. Thurston, G., McLean, J. W., Rizen, M., Baluk, P., Haskell, A., Murphy, T. J., Hanahan, D., and McDonald, D. M. Cationic liposomes target angiogenic endothelial cells in tumors and chronic inflammation in mice. J. Clin. Investig., *101:* 1401–1413, 1998.
48. Muggia, F., and Hamilton, A. Phase III data on Caelyx in ovarian cancer. Eur. J. Cancer, *37* (Suppl. 9)*:* S15–S18, 2001.

Vascular Damage and Anti-angiogenic Effects of Tumor Vessel-Targeted Liposomal Chemotherapy

Fabio Pastorino, Chiara Brignole, Danilo Marimpietri, et al.

Cancer Res 2003;63:7400-7409.